HIGH FREQUENCY MONITORING OF SWASH HYDRO-MORPHODYNAMICS ON A REFLECTIVE BEACH (GRAND POPO, BENIN): A NEW METHOD

Raimundo Ibaceta[1], Rafael Almar[2], Jean-Pierre Lefebvre[2], Trinity Mensah-Senoo[3] and Wahab Sowah Layrea[3].

A new remote sensing video-based method for measuring rapid variations of the bed elevation and free-surface in the swash zone is tested on a steep reflective beach at Grand Popo. The key assumption is that the free-surface has a distinguishable optical signature with respect to the bed level. This new set up enables a high frequency description of the wave transformation, dissipation and reflection in the swash zone as well as the variations of the bed evolution at the wave-by-wave scale. At a more integrated scale, a good correlation is found between the offshore reflected energy measured by an ADCP, the incident offshore wave characteristics and the swash local morphology, suggesting the importance of the swash dynamics on the energy reflection mechanism.

Keywords: Video pole technique, remote sensing, image processing, swash zone dynamics, low tide terrace, incoming and outgoing wave energy, individual wave scale, shoreface rapid evolution.

Introduction

The swash zone is a very dynamic zone of the nearshore experiencing large levels of sediment transport, turbulence and large rates of morphological changes from the short term (swash-to-swash scale) to longer term events (tidal cycle). Last reviews regarding the swash zone can be found in the work by Butt and Rusell 2000; Elfrink and Baldock 2002; Masselink and Puleo 2006; Brocchini and Baldock 2008. Though their importance, the processes associated to the energy transfer between short and long waves and beach reflection remains unknown; the last being crucial to understand how the swash affects the long wave behavior, the standing wave patterns and the interaction with the beach morphology (Masselink and Puleo 2006). Beach reflection has been studied using laboratory data, showing a link between energy reflection and the ratio of wave steepness to beach slope, which can be described in terms of the Iribarren number or surf-similarity parameter ξ (Iribarren and Nogales, 1949, see also Battjes et al., 1974). However, field observations have shown that these predictions do not match well for irregular waves and complex morphology (Elgar et. al, 1994). Recent works have shown the role played by the swash slope on beach energy reflection; for example, studies using laboratory and numerical data (Almar et al., 2012) have suggested the major control of the swash slope on the outgoing reflected wave energy, with the swash playing the role of a low-pass band filter in which the flatter is the beach, the lower frequency is the outgoing energy component.

In the swash zone, the degree of our knowledge decreases when going down to small scales towards individual events. It is thus necessary to properly quantify and predict the sediment transport and beach face evolution in the swash zone at high frequencies (see for example Blenkinsopp et al., 2011), in particular the high role played by the interaction between uprushes and backwashes on the net sediment transport (swash-by-swash event impact). For a sequence of waves approaching the beach, the degree of swash interactions depends on the ratio between the natural period of individual swash events T_s and the incident wave period T (Brocchini and Baldock 2008). For $T>T_s$ little or no interactions occurs, where swash interaction occur between incident waves and the uprush or backwash of preceding waves for $T_s > T$. This interaction may generate a range of scales of new motion such as hydraulic jumps, turbulence and high degree of energy dissipation.

Previous work on swash free-surface and bed elevation measurement at high frequencies have obtained data using a variety of techniques. The methods used so far include measurements array using ultrasonic altimeters (Turner et al. 2008; Masselink et al. 2009) and higher spatial resolution instruments as industrial LIDAR (Blenkinsopp et al. 2010; Vousdoukas et al. 2014). Both methods have shown a good description of the swash free surface and bed level measurements but there's still a lack of certain low cost method capable of measuring the same hydro- morphodynamics data. For

[1] Departamento de Obras Civiles, Universidad Técnica Federico Santa María, Valparaíso, Chile. raimundo.ibaceta@alumnos.usm.cl.
[2] UMR LEGOS (IRD-CNRS-CNES-University of Toulouse III), Toulouse, France. rafael.almar@ird.fr, jean-pierre.lefebvre@ird.fr.
[3] University of Ghana, Ghana. tri_box3@hotmail.com, sowah_layrea@yahoo.com.

instance, both instruments explained above have a cost of the order of US$5000 (LIDAR) and US$450 for each ultrasonic bed level sensor.

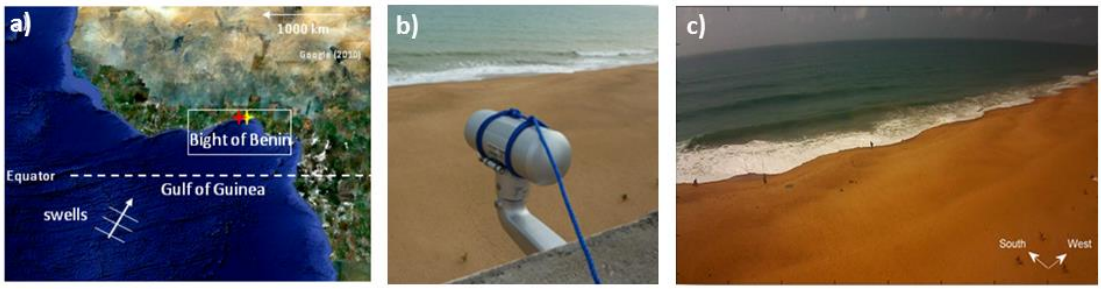

Figure 1. a) Bight of Benin. b) Long term video system. c) Overview of Grand Popo beach taken by the long term system video camera.

In this paper, we introduce and show the capabilities of a new remote sensing technique based on video poles to measure the swash free-surface and bed evolution at high frequencies. We first present the study site and the experimental setup, which includes the description of the new method. Preliminary results on swash zone elevation variations are shown for different types of individual swash events. We present results based on offshore ADCP measurements of wave energy reflection and its relation with the local swash zone slope. Finally, some concluding remarks and perspectives on the use of the video pole technique in better understanding swash-induced energy reflection are given.

Study Site, Instruments and Measurements

A field study was conducted from 17 to 28 February 2013 at Grand Popo beach (6.2°N, 1.7°E, Fig. 1a; see Almar et al., 2014a) in Benin, Gulf of Guinea, midway (80 km) between Cotonou (Benin's capital) and Lomé (Togo). Grand Popo is representative of the beaches of the bight of Benin, presenting a storm free open wavedominated (ECMWF 1957-2013 annual wave average H_s=1.36 m, T_p=9.4 s, *Dir* = S-SW) and microtidal environment (0.3 to 1.8 m for neap and spring tidal ranges respectively) exposed to long swells generated at high latitudes in the South Atlantic with an oblique incidence of 15° to 20°. The beach presents an alongshore uniform low-tide terrace and a steep high tide reflective part characterized by a persistent cuspate pattern (L ~ 30 m). Sediment is medium sized (D_{50}=0.6 mm) and an eastward littoral drift of 400 up to 1000 m^3/*year* has been reported in the literature (Blivi et al. 2002), driven by the typical oblique incident waves.

The deployments were designed both to measure beach changes continuously from the short timescale (swash event) to longer time scale (~tide). The swash zone was instrumented using a new low cost remote sensing monitoring system (introduced in next section). Incident and reflected energy were measured with an ADCP (RDI WORKHOUSE) moored offshore at 10 m depth. Other measurements carried out include surf zone currents by means of human drifters (Castelle et al. 2014), a bathymetric survey conducted the last day of the experiment using an echosounder (GARMIN GPS MAP526S) and daily shoreface surveys (Senechal et al. 2014) using a GPS (TOPCON). Finally, a permanent long-term video system (camera VIPOTEK IP7361, 1600x1200 pixels) was deployed at 15 m above MSL at the top of a semaphore of the Benin Navy, at 80 m from the shore (Figs. 1b,c and 2a).

Swash measurements and data processing

The swash experimental setup consisted in 2 cross-shore transects (Fig. 2a) of black-painted wooden poles (Figs. 2b,c), at the horn and bay of a cusp system. Each transect had up to 7 poles positioned every 4 m approximately. For each transect, a high definition camera (SONY HDR-CX 250, 1920x1080 pixels) was used to monitor the swash zone with an acquisition rate of 25 Hz during 5 days (from 22 to 26 Feb. 2013) for an almost complete tidal cycle each day. Each transect of the video pole method (camera + poles) costs about US$250. Pole's location (blue points in Fig. 3a) are automatically extracted from the images and recomputed every 10 s to cope with possible small movements of both camera and poles.

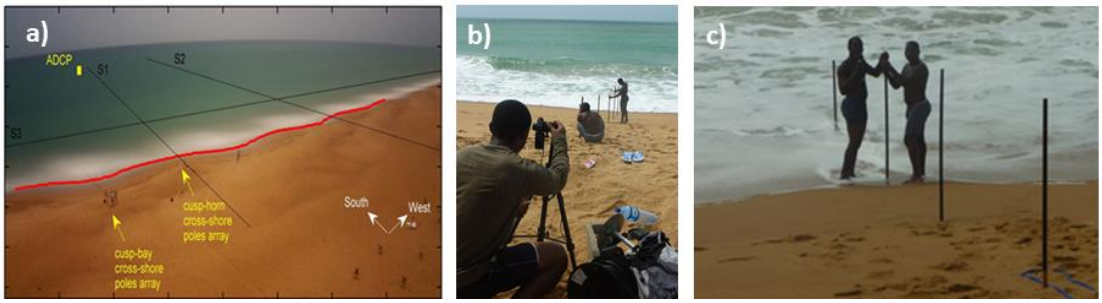

Figure 2. a) Long term camera overview. b) Poles and camera deployment to measure swash hydro-morphodynamics. c) Pole's deployment detail.

Timestack images are generated for each pole along its vertical direction as shown in Fig. 3b. RGB(Red, Green, Blue) timestacks images are converted into binary matrix (Figs. 3b,c,d). The automatic detection of the bed and water interface relies on the identification of abrupt change of pixel intensity at water-pole and bed-pole transitions. Small differences between detected bed and real bed level are corrected manually when necessary. A final representation of 3 swash events timestack for one single pole is shown in Fig. 3e. The rectification from pixel coordinates to real world coordinates is done considering the thickness of reference of known width; the pole's diameter in this case (3 cm). The vertical levels are georeferenced using the pole's top positions, measured using an RTK GPS right before the beginning of the swash measurements.

A complete validation of this new method is part of an ongoing work carried out comparing the swash free-surface and bed level measurements with conventional instruments such as pressure sensors, LIDAR and ultrasonic bed level sensors. A comparison with LIDAR and pressure sensors can be found in Almar et al. 2014b,c. A comparison with GPS measurements of the bed level is presented in the next section.

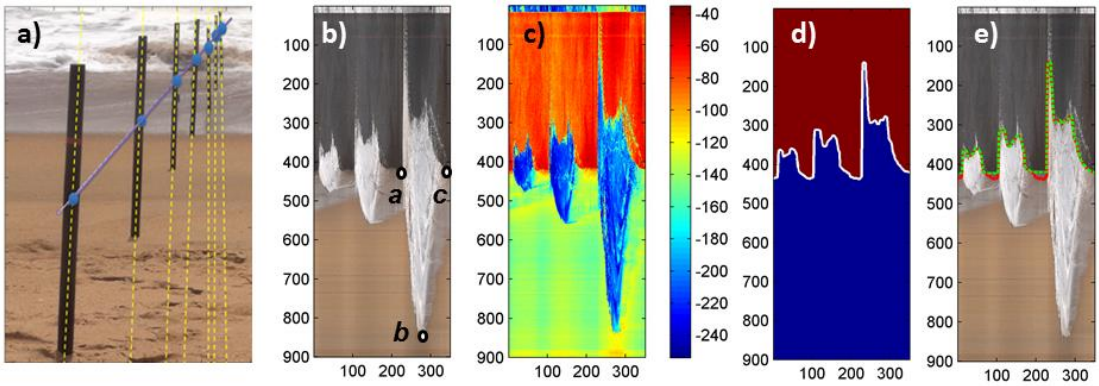

Figure 3. a) Typical camera overview. The purple line represents a stack line used to detect every pole position automatically. b) Original timestack of 3 swash events (app. 300 pixels representing 300 extracted lines.)
c) Pixel intensity. d) Binary matrix e)Timestack with (red) detected contour and (green dashed) corrected countour.

RESULTS

Comparison of the bed evolution with GPS measurements

A comparison is done between the bed level evolution at 3 poles using co-localized GPS measurements for a 90 min time-series where, every single swash event impact was detected from video. A -single swash event is identified using the definition proposed by Blenkinsopp et al. (2011); the elevation between two different intervals of constant height representing the dry bed level. With this definition, swash events are automatically detected identifying the initial and final time and elevation A(t_a,z_a) and C(t_c,z_c), respectively, as shown in Figs. 4a,b,c. The bed level variation using both methods is computed using the following expression, where τ is the period of time considered (90 minutes) and n is the number of swash events detected over τ.

$$\Delta z_{video} = \sum_{i=1}^{n} (z_{ci} - z_{ai}) \quad (1)$$

The bed level change at 3 poles location using GPS is measured twice over τ and compared with the video measurements, achieving the results presented in Table 1.

Table 1. Comparison between GPS and video pole measurements of the bed evolution.

pole	n	$\Delta z_{\tau\, video}$ (cm)	$\Delta z_{\tau\, GPS}$ (cm)
6	41	-0.9	-1
7	109	0.8	1
8	205	5.7	5

As shown in the Table 1, a good agreement between erosion (pole 6) and accretion patterns (pole 7 and 8) are found.

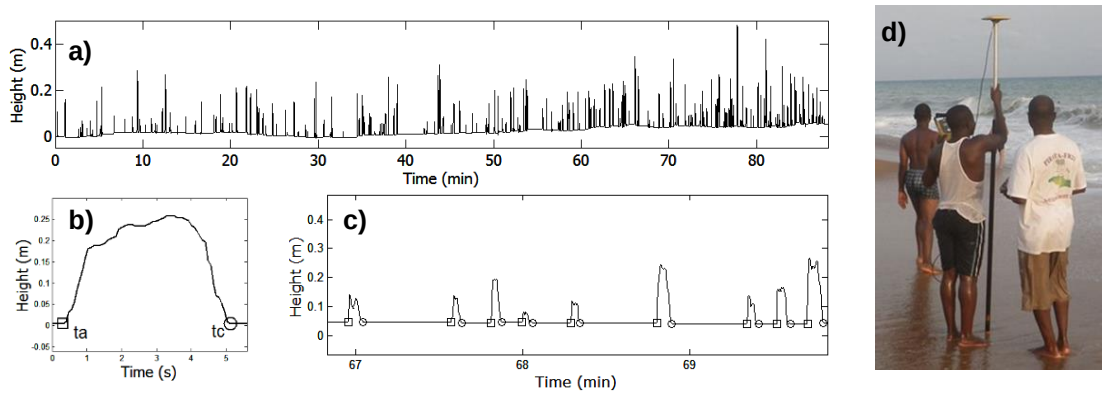

Figure 4. a) 90 minutes timeseries for a single pole. b) Identification of swash events, initial and final times. c) Detail of 9 swash events. d) GPS measurements of the bed elevation.

Description of swash events

As an illustration of the new technique, some typical swash events observed during the field study were studied with reference to the Figures 5a and 5b and with the type of swash events described by Brocchini and Baldock (2008). Three characteristics times in a swash events can be deducted from a time stack; the time when the uprush reaches a given pole (t_a), the time (t_b) corresponding to the maximum reach of the swash (run up) and the end (t_c) of a swash event for the corresponding pole, as shown in figure 3b.

- Free swash event (Fig. 5b, 13:20:54 – 13:21:05): These events are characterized by a regular shape with an initial bore travelling shoreward, conserving its shape up to the point of maximum extension as its height and velocity decrease. Flow reversal may begin prior to the time of maximum run up, due to gravity and without being influenced by the next incident wave.
- Swash interactions (Fig. 5b, 13:20:32 – 13:20:45): The interaction between a backwash and the next uprush can happen when Ts > T. This interaction tends to hinder the uprush extension concentrating high levels of turbulence over a narrow area. As the hindering by the backwash ceases, the uprush propagates shoreward but along a reduced extensions since the energy has been dissipated during the interaction. This mechanism was observed several times and it is related to the beach steep profile which produces interaction between uprushes and backwashes and not following uprushes, responsible of the typical infragravity motion of gently sloping beaches.

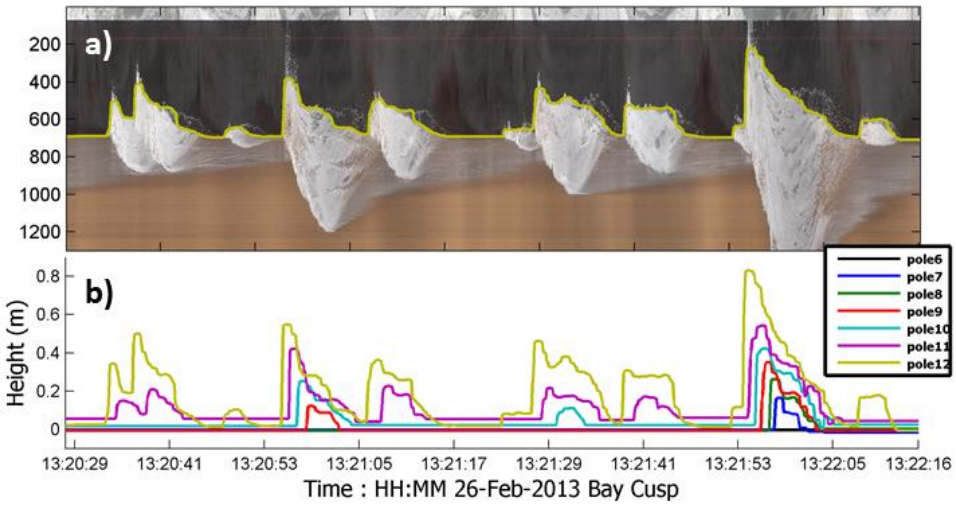

Figure 5. a) Time stack of the pole 12 (located most offshore) and its corresponding free-surface and bed elevation detection. b) Propagation of the bore along the cross-shore extension.

- Two dimensional interaction (Fig. 5b, 13:22:08 – 13:22:13): It was common to see interactions coming from the beach cusp-horn as an alongshore flow. This is observed on the elevation time series as quasi uniform shape and constant elevation events because of the alongshore local slope nearly constant on the direction of this secondary interaction. While the lower part of the beach was alongshore uniform, it was rather 3D and irregular at the upper shoreface due to the presence of cusps which induced this kind of 2D interactions.

The Fig. 6 shows 6-min timestacks for transect at the beach cusp bay (Fig. 6a) and horn (Fig. 6b) at the same moments. Upper panels show a cross-shore timestack generated by extracting a line along the cross-shore direction passing beside the pole's bottom. Lower 3 images represent the cross-shore propagation of the bore for 3 poles at both alongshore positions. It can be seen on the cross-shore timestacks that same offshore hydrodynamics produce different run up extensions. This induces a different behavior of the change of bed level (Δz at swash event scale) along the horn and bay profiles. For instance, individual values of Δz follow different patterns along the cross-shore direction and throughout the alongshore direction for moments of time between 1 and 2 min. Our studies show the crucial importance of swash interactions, bore celerity and local bed level explaining the variability of Δz as pointed out by Ibaceta et al. (2014). The latter will be further investigated.

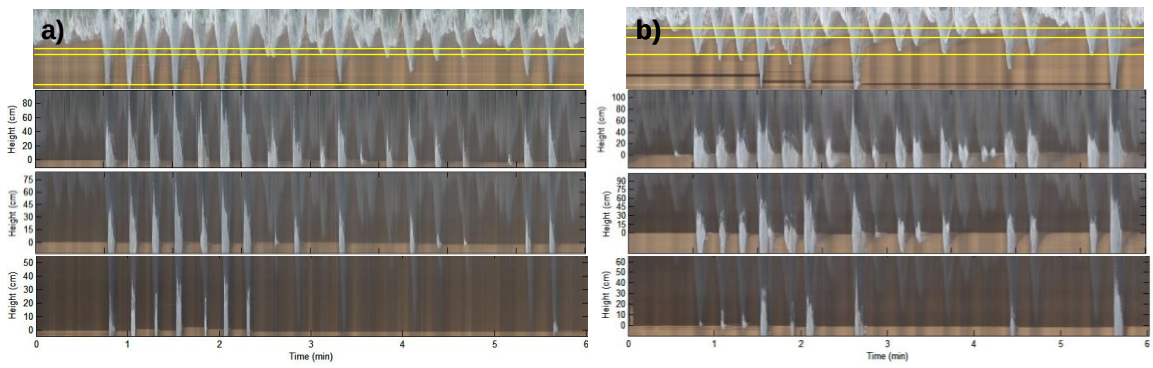

Figure 6. a) Cross-shore timestack at the beach cusp (upper panel) and cross-shore bore propagation for 3 consecutive video poles. Yellow lines stand for the cross-shore pole's position. b) Cross-shore timestack at the beach horn (upper panel) and cross-shore bore propagation for 3 consecutive video poles.

Swash slope variation

It is possible to measure the variation of the shoreface with the video pole method. Fig. 7a shows the shoreface evolution over 200 min along 6 poles (vertical black grids). The lower part of the beach experiences accretion and the upper part erosion patterns. Fig. 7b presents the same procedure for a longer time scale, where the evolution of the bed level during 6 hours for pole 7 (most shoreward) to pole 11 (most seaward) is shown. Shoreward poles experience net erosion whereas the seaward poles experience a net accretion pattern, resulting in a decrease of the mean beach slope.

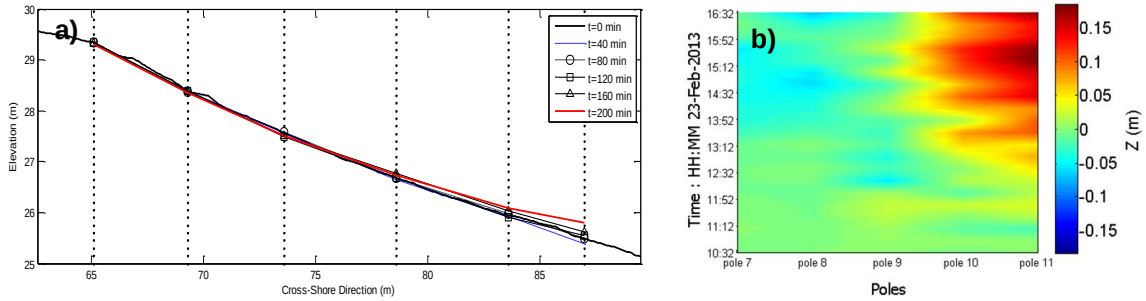

Figure 7. a) Beach profile variation over 200 min measured at pole's position. Solid black line stands for t = 0 min measured with GPS and solid red line stands for the final profile measured after 200 min with video poles. Vertical points stand for the pole's positions. Even though the shorefaces are shown every 40 min, the video pole method is able to represent its variation at higher frequencies (swash-to-swash scale). b) Variation of the bed level along a cross-shore transect. Values between every pole are interpolated.

Role of the swash on energy reflection

Fig. 8a shows a time series of outgoing to the incident energy ratio E_{out}/E_{inc} measured by the ADCP. A visual analysis of this figure evidences that most of the local peaks of the energy ratio coincide with high tide measured with ADCP (series not shown here). This suggests a relation between the swash local morphology and the energy ratio, since Grand Popo has a typical steep reflective upper shoreface and a rather dissipative gently sloping low tide terrace, as shown in Fig. 8b.

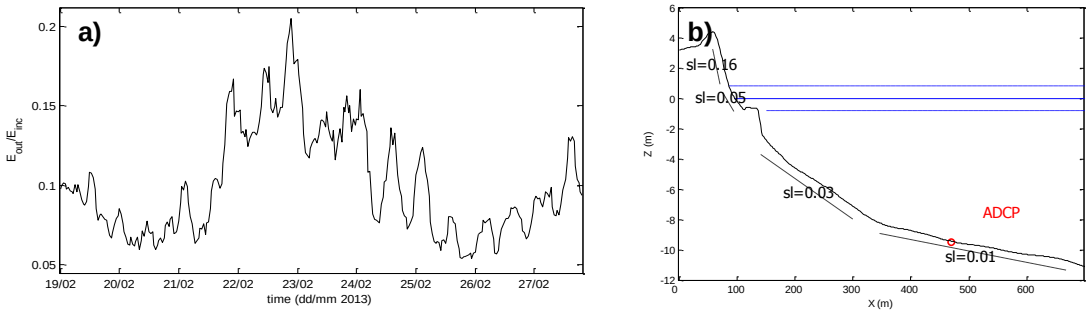

Figure 8. a) Timeseries of the outgoing energy to the incident energy over the experiment extension. b) Alongshore averaged profile for the complete experiment, measured with GPS and echosounder. Z=0 m is the mean water level (solid blue line) and dashed blue lines are spring high and low tide levels.

With this in mind and based on previous knowledge of the Iribarren number as an important parameter on beach energy reflection, we investigate the relation between the outgoing energy and hydro-morphodynamics parameters. A multilinear regression is used in order to describe the energy reflection in terms of the local morphology and the incident energy. The model is defined as $Y=b_1X_1 + b_2X_2 + \ldots + b_nX_n$,where b_n are the regression coefficients, X_n are the input parameter timeseries and Y the target timeseries to be modeled. A linear reconstruction of the parameter E_{out}/E_{inc} is done in terms of a proposed modification of the Iribarren number, using the local swash slope β instead of the surf zone slope. The modified Iribarren number was calculated using ADCP measurements of the offshore incident energy and the GPS measurements of the swash slope. Figure 9a shows the linear reconstruction and the figure 9b a scatter plot of the energy ratio to the local Iribarren number (R^2=0.78), underlying a good agreement and consequently the high role played by the swash on the energy reflection.

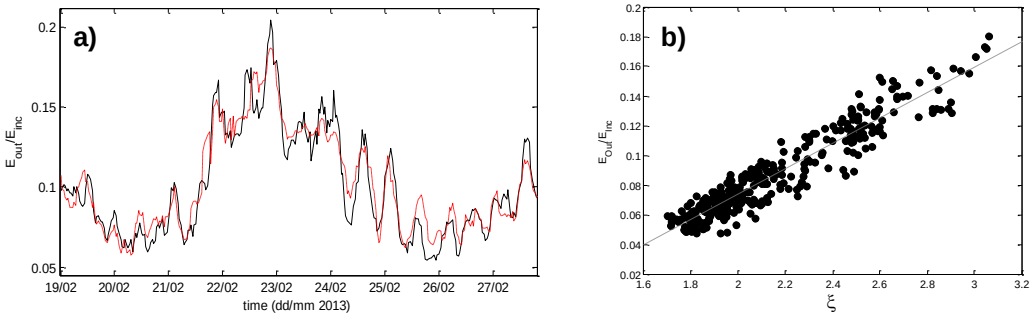

Figure 9. a) Timeseries of the outgoing energy to the incident energy (black) and the corresponding linear reconstruction in terms of the local modified Iribarren number (red). b) Scatter plot of the energy ratio to the local Iribarren number.

Conclusions

The new video pole technique provides a good description of wave transformation and shoreface evolution at the wave-by-wave scale and at longer scales (hours). Advantages of this new method include its very low cost, easy deployment setting and accuracy ($0(10^{-3})$ m). The possibility of having the raw video recorded also facilitates the understanding of the physical phenomena involved when studying the time series of bed level and free-surface elevation since it is possible to check the images when necessary. The main disadvantage of the method is the limited spatial resolution which depends on the number of poles deployed.

A good agreement is found between the local swash slope and the incident and reflected energy measured offshore, suggesting the important role played by the swash on the energy reflection. This is of high importance for nearshore energy balance. For instance, most of the regional nearshore models do not include wave reflection, which in turn might result in underestimating the value of Hs up to 10% as pointed out by Ardhuin and Roland 2012. As a consequence, if swash zone is key in energy reflection, further research will focus in having an estimation of this swash slope by means of equilibrium concepts between hydrodynamics and local morphodynamics.

Future investigation involving the new method includes data collected during a second field experiment conducted in March 2014 at Grand Popo, where up to 18 poles positioned every 1 (m) were deployed, allowing a better macro scale description of the wave transformation and impact on beach morphology. A micro current profiler was deployed to measure high frequency velocities and suspended sediment transport in complement to video measurements. Moreover, a complete validation of the method is being carried out using data of different sandy beaches such as Nha Thrang, Vietnam (wind-waves dominated, intermediate beach) and Mataquito and Reñaca in Chile, a dissipative-intermediate and reflective beach, respectively, both exposed to long energetic swells.

Acknowledgements

The field study was funded by the INSU LEFE and EC2CO programs, the IRD and the UNESCO co-chair CIPMA. RI thanks the CNRS' grant to do an internship at LEGOS and for the expenses needed to attend the ICCE 2014. RI thanks also the Chilean project FONDAP 2011 No 15110017 (CIGIDEN).

References

Almar R., Cienfuegos R., Gonzalez E., Catalán P., Michallet H., Bonneton P., Castelle B and Suarez L., 2012. Barred-beach morphological control in infragravity motion. *Proceedings of the International Conference on Coastal Engineering*, 1-6 July 2012, Santander, Spain.

Almar R., Hounkonnou N., Anthony E., Castelle B., Senechal N., Laibi R., Mensah-Senoo T., Degbe G., Quenum M., Dorel M., Chuchla R., Lefebvre J.P., du Penhoat Y., Layrea W.S., Zodehougan G., Sohou Z., Addo K., Ibaceta R. and Kestenare E., 2014a. The Grand Popo beach 2013 experiment, Benin, West, Africa: from short timescale processes to their integrated impact over long-term coastal evolution". *Proceedings of the International Coastal Symposium 2014*, Durban, South Africa.

Almar R., Catalán P., Ibaceta R., Blenkinsopp C., Cienfuegos R., Villagrán M., Aguilera J.C. and

Castelle B., 2014b. Swash zone based reflection during energetic wave conditions at a dissipative beach : toward a wave-by-wave approach. *Proceedings of the 34th Conference on Coastal Engineering*, Seoul, South Korea.

Almar, R., Bonneton P., Bonneton N., Lefebvre J.P., Dinh V.U., Nguyen T.V., Le T.B., Nguyen V.D., 2014. Swash hydro-morphodynamics at the low-tide terrace beach during post-typhoon recovery period, Nha Trang bay, Vietnam. *19th IAHR-APD 2014 Congress.* 21-24 September 2014, Water Resources University, Hanoi, Vietnam

Ardhuin F. and A. Roland. 2012. Coastal wave reflection, directional spread, and seismoacoustic noise sources. *Journal Of Geophysical Research-oceans*, 117(C00J20), 16pp.

Battjes, J.A., 1974. Surf similarity. *Proceedings of the 14th International Conference of Coastal Engineering (American Society of Civil Engineers),*466-480

Blenkinsopp C., M. Mole, I. Turner, W. Peirson. 2010. Measurements of time-varying free-surface profile across the swash zone obtained using an industrial LIDAR. *Coastal Engineering* 57 (2010).1059-1065.

Blenkinsopp C., Turner I., Masselink G. and Rusell P. 2011. Swash zone sediment fluxes: field observations. *Coastal engineering*, Vol. 58(1), 28-44.

Blivi A., Anthony E. and Oyédé L. 2002. Sand barrier development in the bight of Benin, West Africa. *Ocean and Coastal Management*, 45, 185-200.

Brocchini M., and Baldock T. 2008. Recent advances in modelling swash zone dynamics: Influences of surf-swash interaction on nearshore hydrodynamics and morphodynamics. *Reviews of Geophysics*, Vol. 46, No. 3.RG3003

Butt T. and Rusell P. 2000. Hydrodynamics and cross-shore sediment transport in the swash-zone of natural beaches; a review. *Journal of Coastal Research* 16 (2), 255-268.

Castelle B., Almar R., Dorel M., Lefebvre J.P., Senechal N., Anthony E., Chuchla R. and du Penhoat Y. 2014. Flash rip dynamics on a high-energy low-tide-terraces beach (Grand Popo, Benin, West Africa), *Proceedings of the 13th International Coastal Symposium*, Durban, South Africa.

Elfrink B. and Baldock T. 2002. Hydrodynamics and sediment transport in the swash zone: a review and perspectives. *Coastal Engineering* 45 (3-4), 149-167.

Elgar, S., Herbers, T.H.C. and Guza R.T., 1994. Reflection of ocean surface gravity waves from a natural beach, J. *Physical. Oceanogr.*, 24(7), 1503-1511

Ibaceta R., Almar R., Lefebvre J-P., Mensah-Senoo T., Laryea W.S., Castelle B., Senechal N., du Penhoat Y., Laibi R. and Hounkonnou N.. 2014. A new high frequency remote sensing based method: application to the swash zone of a very high reflective beach under high energetic conditions (Grand Popo, Benin), *Actes des XIIIèmes Journées Nationales Génie Côtier - Génie Civil*, Dunkerque 2014, Paralia Editions.

Iribarren C. and Nogales C., 1949. *Protection des Ports. XVIIth International Navigation Congress*, Section II, Communication,pp. 31-80.

Masselink G., and Puleo J., 2006. Swash-Zone Morphodynamics. *Continental Shelf Research*, Vol. 26, 661-680.

Masselink G., Russell P., Turner I and Blenkinsopp C., 2009. Net sediment transport and morphological change in the swash zone of a high-energy sandy beach over tidal cycle and swash event time scales. *Marine Geology* 257, 18-35.

Senechal N., Laibi R., Almar R., Castelle B., Biausque M., Lefebvre J.P., Anthony J., Dorel M., Chucla R., Hounkonnou N. and du Penhoat Y., 2014. Observed destruction of a beach cusp system in presence of a doublecoupled cusp system : the example of Grand Popo, Benin. *Proceedings of the International Coastal Symposium 2014*, Durban, South Africa.

Turner I.L., Rusell P. and Butt T., 2008. Measurement of wave-by-wave bed levels in the swash zone. *Coastal Engineering* 55 (12), 1237-1242.

Vousdoukas M.I., Kirupakaramoorthy T., Oumeraci H., de la Torre M., Wubbold F., Wagner B., Schimmels S., 2014. The role of combined laser scanning and video techniques in monitoring wave-by-wave swash zone processes, *Coastal Engineering* 83, 150-165, ISSN 0378-3839.